TOWARDS DENSE MOTION ESTIMATION IN LIGHT AND ELECTRON MICROSCOPY

Luis Pizarro[1], *José Delpiano*[2], *Paul Aljabar*[1], *Javier Ruiz-del-Solar*[2], *Daniel Rueckert*[1]

[1]Department of Computing, Imperial College London, 180 Queen's Gate, SW7 2AZ, London, UK
[2]Department of Electrical Engineering, University of Chile, Av. Tupper 2007, Santiago, Chile

ABSTRACT

Motion estimation, also known as optic flow, refers to the process of determining a 2D displacement field that aligns two images. Most methods that estimate motion or deformation fields in biological image sequences rely on *sparse*, distinct features (landmarks). Going a step forward, we are interested in methods to compute *dense* deformation fields (for all pixels). In this paper we compare two of such frameworks: the B-splines based *free-form deformation* (FFD) approach, which is well-known in medical image registration; and the *combined local-global* (CLG) approach, a popular optic flow method in computer vision. We test both methods on synthetic and real image sequences obtained by confocal light microscopy and by scanning electron microscopy, showing their performance in terms of accuracy and computational cost. As an alternative to traditional sparse techniques, the estimation of dense motion fields would allow tackling other related problems with sub-pixel precision, for example, the segmentation and classification of different biological structures according to their local motion, trajectory, growth and development.

Index Terms— Motion estimation, optic flow, deformation field, light microscopy, electron microscopy

1. INTRODUCTION

Numerous studies in bioimaging rely on tracking algorithms to follow the displacement of certain objects such as cells, neurons, membranes, etc. Due to the large size of standard biological data sets such algorithms usually attempt to trace only a few distinct landmarks that are manually or semi-automatically chosen. For instance, [1] compares several registration methods for tracking nuclei centres in confocal microscopy images, while in [2] a few image patches are manually chosen to accelerate the registration process of electron microscopy images. Nevertheless, there are no really efficient approaches for biological imaging that consider the estimation of dense displacement or deformation fields. This is of particular interest for many studies and applications since it would allow, with sub-pixel precision, a much more accurate description and understanding of the underlying biological processes observed under the microscope.

The goal of this paper is to explore two techniques originated in other research areas for computing dense deformation fields in bioimaging . The first one is the B-splines based free-form deformation (FFD) approach proposed by Rueckert *et al.* [3] in the context of medical image registration. The second one is the combined-local and global (CLG) method of Bruhn *et al.* [4] proposed in the context of optic flow in computer vision. After describing both methods (Section 2), we test their capabilities to estimate dense motion fields on both light and electron microscopy data sets under synthetic and real conditions (Section 3). We discuss how these methods can be utilised for specific applications in chemotactic processes and for studying blood vessel development. Finally, we summarise our contributions and discuss future work (Section 4).

2. METHODS

2.1. Free-Form Deformation Approach

The goal of the B-splines based free-form deformation (FFD) approach for non-rigid registration [3] is to estimate an optimal transformation $\mathbf{T} : \Omega \supset (x, y) \rightarrow (x', y')$ that maps any point in an image sequence $I_t(x, y)$ at time t onto its corresponding point in the reference image $I_{t_0}(x', y')$ taken at time t_0. The mapping $\mathbf{T}$ minimises the cost functional

$$C(\Phi) = C_{similarity}(I_{t_0}, \mathbf{T}(I_t)) + \lambda\, C_{smooth}(\mathbf{T})\,. \qquad (1)$$

A common and powerful similarity measure $C_{similarity}$ is the normalised mutual information [5], mainly used when registering two different imaging modalities. That is not the case in this paper, so we instead choose

$$C_{similarity}(I_{t_0}, \mathbf{T}(I_t)) = \frac{1}{n} \int \left(I_{t_0} - \mathbf{T}(I_t)\right)^2 d\Omega \qquad (2)$$

that measures the intensity similarity between the images, with n the number of pixels. The term

$$C_{smooth}(\mathbf{T}) = \frac{1}{n} \int \left(\frac{\partial^2 \mathbf{T}}{\partial x^2}\right)^2 + \left(\frac{\partial^2 \mathbf{T}}{\partial y^2}\right)^2 + \left(\frac{\partial^2 \mathbf{T}}{\partial z^2}\right)^2 d\Omega \qquad (3)$$

penalises deviations from smoothness in the deformation field. The weighting parameter λ in (1) defines the tradeoff between the similarity and the smoothness term.

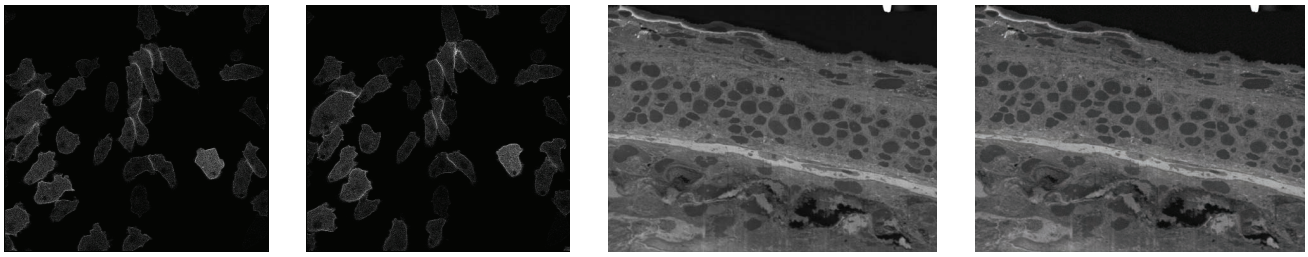

(a) LM frame 1 (b) LM frame 2 (c) EM slice 1 (d) EM slice 2

Fig. 1. (a)-(b) subsequent frames of an image sequence obtained by confocal light microscopy (LM). (c)-(d) show two slices of a 3D data set collected by scanning electron microscopy (EM). See details in Subsection 3.1.

For the sake of simplicity we disregard global affine transformations. In this case, the mapping $\mathbf{T}$ accounts for local deformations occurring all over the image domain and is defined as a B-spline function on a mesh Φ of equidistant control points (CPs). Estimating the location of the CPs gives the desired transformation map. Increasing the number of CPs allows for computing dense deformation fields more accurately. The functional (1) is minimised by gradient descent using a multiresolution strategy [3].

2.2. Combined Local-Global Approach

The combined local-global (CLG) approach [4] is formulated as a variational method that estimates the motion vector $\mathbf{w} := (u, v, 1)^\top$ at each pixel location by minimising the energy functional

$$E(\mathbf{w}) = E_{similarity} + \lambda\, E_{smooth}\,, \tag{4}$$

where the term

$$E_{similarity} = \int \mathbf{w}^\top J_\rho(\nabla_3 I)\, \mathbf{w}\, d\Omega \tag{5}$$

measures the similarity between two consecutive frames in an image sequence. Here $\nabla_3 := (\partial x, \partial y, \partial t)^\top$ is the spatio-temporal gradient and $J_\rho(\nabla_3 I) := K_\rho * (\nabla_3 I \nabla_3 I^\top)$ is a second-order tensor which integrates local directional information from neighbouring pixels by convolution with a Gaussian kernel K_ρ of width ρ. This similarity term derives from the local method of Lucas and Kanade [6]. The smoothness term

$$E_{smooth} = \int |\nabla u|^2 + |\nabla v|^2\, d\Omega \tag{6}$$

enforces regularity in the displacement field $\mathbf{w}$. The first (global) variational optic flow method is due to Horn and Schunck [7], which uses this regularisation term together with the similarity (5) with $\rho = 0$.

The CLG approach is therefore a combination between the local Lucas-Kanade method and the global Horn-Schunck approach. Moreover, note that the quadratic terms in (4) makes this a linear method with a unique solution. There exist a non-linear formulation of the CLG approach with non-quadratic penalisers. However, we do not consider it here as we compare this method with the FFD approach that also utilises quadratic penalisers. The energy functional (4) is minimised by solving its corresponding Euler-Lagrange equations. These equations generate a large system of equations that is solved very efficiently by full multigrid strategies [8].

3. EXPERIMENTS

3.1. Data Sets

Fig. 1(a) and Fig. 1(b) display two consecutive frames of an image sequence obtained by confocal light microscopy [9] showing the movement of chemotactic cells. One can observe that these cells undergo large motions between subsequent frames, which were taken every 20 seconds. In this particular application, it is interesting to compute a dense motion field to study the way these cells move, collide and group, which allows an accurate characterisation of the chemotactic process. Fig. 1(c) and Fig. 1(d) exhibit two slices of a 3D data set collected by focused ion beam/scanning electron microscopy [10] showing blood vessels of a zebrafish embryo at high resolution (72nm). A dense alignment of these slices would allow an accurate 3D reconstruction and segmentation of neurons as the basis for studying blood vessel development.

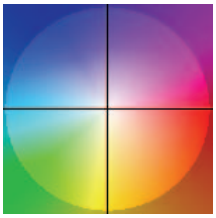

Fig. 2. Colour code representing a motion vector at each pixel location. The vector's angle (with x-axis) specifies the colour and the vector's magnitude indicates the colour intensity.

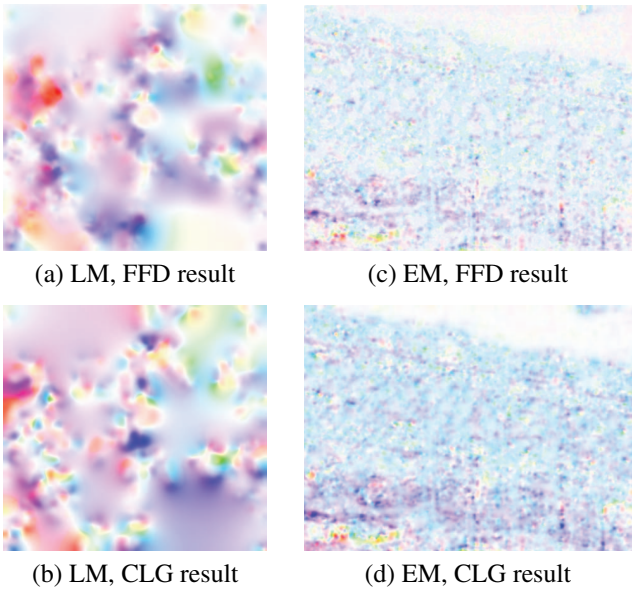

(a) LM, FFD result (c) EM, FFD result

(b) LM, CLG result (d) EM, CLG result

Fig. 3. Displacement fields computed with both FFD and CLG methods for the LM and EM data sets shown in Fig. 1.

3.2. Results

We now test both methods, FFD and CLG, to densely estimate the displacement fields between the image pairs (a)-(b) and (c)-(d) shown in Fig. 1. For visualisation purposes, we represent the displacement vector at each pixel location according to the colour scheme shown in Fig. 2.

Fig. 3(a) and Fig. 3(b) show the FFD and CLG results for the light microscopy (LM) pair (a)-(b) from Fig. 1. Despite the fact that the cells in these subsequent frames exhibit a large deformation, both methods are able to deliver reasonable dense results. The blurry artifacts appear at the background where there is little or no motion at all. This is more pronounced in the CLG method, which is less able to track largely deforming shapes than the FFD method. Interestingly, by looking at the colour maps it is possible to infer the directions along which the cells are moving as well as the magnitude of the displacements. This is specially useful to characterise the chemotactic process the cells are going through.

Fig. 3(c) and Fig. 3(d) show the FFD and CLG results for the electron microscopy (EM) pair (c)-(d) from Fig. 1. In this case, CLG seems more accurate than the FFD. The former approach provides sharper results and less artifacts at the motionless areas. This could happen due to the amount of FFD's control points, which had to be reduced to 1/5 of the pixel resolution to obtain results within an acceptable time frame. The CLG method on the other hand is more suitable when the deformation field is constrained to a few pixels in magnitude as it occurs in 3D EM data. It is important to note that thanks to the dense estimation of displacement vectors

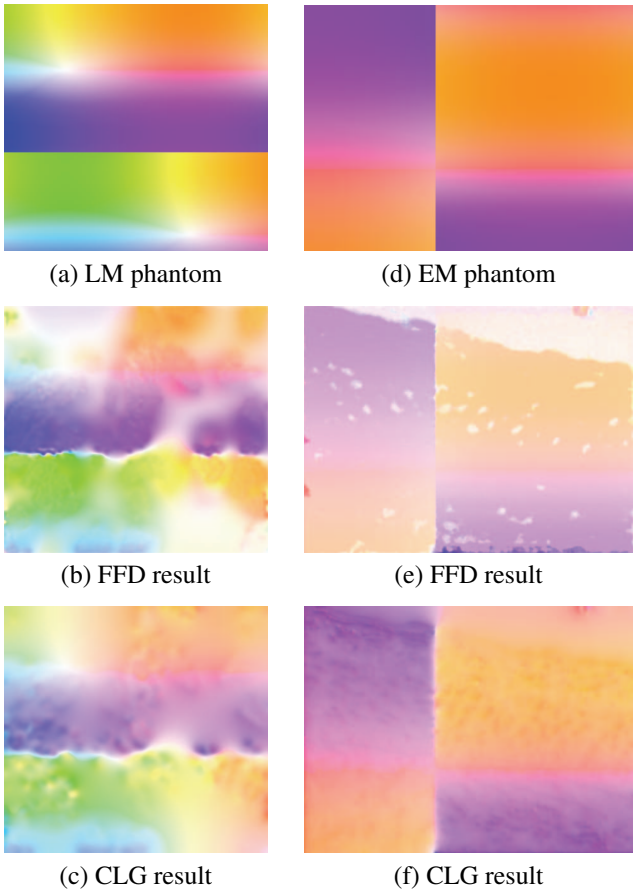

(a) LM phantom (d) EM phantom

(b) FFD result (e) FFD result

(c) CLG result (f) CLG result

Fig. 4. Synthetically generated displacement fields applied to both LM and EM data sets. Displayed results computed with the FFD and the CLG method.

one could be able to determine groups of pixels moving coherently, which can be associated to different types of tissue for segmentation purposes.

To have a better intuition about the way the FFD and CLG methods work, we generate synthetic deformation fields (phantoms) on both LM and EM data sets which are shown in Fig. 4(a) and Fig. 4(d), respectively. The displacements were created following two sinusoidal waves with varied wavelengths and phases. This produces deformation fields with soft and hard discontinuities which we applied to the first frame/slice of each data set. We then registered the original and the deformed images with both methods. The results shown in Fig. 4 suggest that both FFD and CLG can partially deal with hard discontinuities, while at soft discontinuities FFD is less accurate than CLG. However, it seems that FFD sometimes delivers a closer estimation of the deformation magnitude. These observations are confirmed by the average errors at estimating the displacement's orientation (colour) and magnitude (intensity) reported in Table 1 as AAE and AEE respectively. Despite those errors, both methods provide

an excellent alternative to compute dense deformation fields in biological imaging. In terms of computational cost, CLG is much faster than FFD, as shown in Table 2. Both approaches were run on a desktop computer (2GHz, 2GB RAM) and implemented in C++ as described in [3, 8].

Table 1. *Average angular error* (AAE, in degrees) / *average end-point error* (AEE, in pixels) of both FFD and CLG methods on our synthetic phantoms.

	LM phantom	EM phantom
FFD	15.39 / 0.73	5.80 / 0.34
CLG	13.25 / 0.91	5.36 / 0.54

Table 2. *Execution time* (in seconds) of both methods FFD and CLG on our synthetic experiments: LM phantom (516×483 pixels), EM phantom (2000×1500 pixels).

	LM phantom	EM phantom
FFD	281	3368
CLG	0.71	12.7

4. DISCUSSION AND CONCLUSIONS

Given the increasing demand for tracking methods able to densely compute displacement/deformation fields, i.e. estimates for each pixel location, in biological imaging, we have investigated the utilisation of two method for that purpose. In particular, we focused on the B-splined based *free-form deformation* (FFD) model, a well-known method for medical image registration, and on the recognised *combined local-global* (CLG) optic flow approach from computer vision.

We have shown that both methods provide an excellent alternative to estimate dense motion fields in data sets obtained by confocal light microscopy and scanning electron microscopy under real and synthetic conditions. In terms of estimation accuracy, the FFD method is more reliable when there are shapes undergoing large deformations between subsequent frames, as it is sometimes the case in light microscopy. The CLG method, however, performs better when the deformation field is composed of subtle, numerous displacements and it has the additional advantage of being much faster than the FFD method.

We have ongoing work on extending our investigations to fully tackle biological data sets in (3D,time) space. Another interesting research direction goes with a non-linear version of the CLG method, that can better cope with motion discontinuities, which is relevant for multiple studies where the image data undergo deformations/displacements along different spatial directions. Finally, having dense motion fields at our disposal allows us now to deal with the related problem of segmenting different biological structures according to their motion, trajectory, growth and development.

5. REFERENCES

[1] B. Lombardot, M. Luengo-Oroz, C. Melani, E. Faure, A. Santos, N. Peyrieras, M. Ledesma-Carbayo, and P. Bourgine, "Evaluation of four 3d non rigid registration methods applied to early zebrafish development sequences," MIAAB Workshop, MICCAI, 2008.

[2] A. Akselrod-Ballin, D. Bock, R. Reid, and S. Warfield, "Accelerating feature based registration using the Johnson-Lindenstrauss Lemma," in *MICCAI 2009*, G.-Z. Yang et al., Ed., vol. 5761 of *Lecture Notes in Computer Science*, pp. 632–639. Springer Berlin, 2009.

[3] D. Rueckert, L.I. Sonoda, C. Hayes, D.L.G. Hill, M.O. Leach, and D.J. Hawkes, "Nonrigid registration using free-form deformations: application to breast MR images," *IEEE Transactions on Medical Imaging*, vol. 18, no. 8, pp. 712–721, 1999.

[4] A. Bruhn, J. Weickert, and C. Schnörr, "Lucas/Kanade meets Horn/Schunck: Combining local and global optic flow methods," *International Journal of Computer Vision*, vol. 61, no. 3, pp. 211–231, 2005.

[5] F. Maes, A. Collignon, D. Vandermeulen, G. Marchal, and P. Suetens, "Multimodality image registration by maximization of mutual information," *IEEE Transactions on Medical Imaging*, vol. 16, no. 2, pp. 187–198, 1997.

[6] B. Lucas and T. Kanade, "An iterative image registration technique with an application to stereo vision," in *Proc. 7th International Joint Conference on Artificial Intelligence*, Vancouver, Canada, 1981, pp. 674–679.

[7] B. Horn and B. Schunck, "Determining optical flow," *Artificial Intelligence*, vol. 17, pp. 185–203, 1981.

[8] A. Bruhn, J. Weickert, T. Kohlberger, and C. Schnörr, "A multigrid platform for real-time motion computation with discontinuity-preserving variational methods," *International Journal of Computer Vision*, vol. 70, no. 3, pp. 257–277, Dec. 2006.

[9] T. Jin, N. Zhang, Y. Long, C.A. Parent, and P.N. Devreotes, "Localization of the G protein complex in living cells during chemotaxis," *Science*, vol. 287, no. 5455, pp. 1034–1036, 2000.

[10] H.E.J. Armer, G. Mariggi, K.M.Y. Png, C. Genoud, A.G. Monteith, A.J. Bushby, H. Gerhardt, and L.M. Collinson, "Imaging transient blood vessel fusion events in zebrafish by correlative volume electron microscopy," *PLoS ONE*, vol. 4, no. 11, pp. e7716, 11 2009.